Aerosol and Air Quality Research, 17: 1244–1255, 2017

ISSN: 1680-8584 print / 2071-1409 online
doi: 10.4209/aaqr.2016.09.0425

A Set-up for Respiratory Tract Deposition Efficiency Measurements (15–5000 nm) and First Results for a Group of Children and Adults

Jenny Rissler[1,2*], Hanna Nicklasson[3], Anders Gudmundsson[2], Per Wollmer[3], Erik Swietlicki[4], Jakob Löndahl[2]

[1] *Chemistry, Materials and Surfaces, SP Technical Research Institute of Sweden, SE-223 70 Lund, Sweden*
[2] *Ergonomics and Aerosol Technology, Lund University, Box 118, SE-221 00 Lund, Sweden*
[3] *Clinical Physiology and Nuclear Medicine, SUS, SE-205 02 Malmö, Sweden*
[4] *Nuclear Physics, Lund University, SE-221 00 Lund, Sweden*

ABSTRACT

Exposure to airborne particulate matter is associated with a number of negative health effects ranging from respiratory diseases to systemic effects and cancer. One important factor for understanding the health effects is the individual variation in the respiratory tract deposition of inhaled particles. In this study, we describe an experimental set-up for size-resolved measurements of the lung deposited fraction of airborne particles, covering the diameter range from 15 to 5000 nm. The set-up includes a system for generating a stable aerosol with a sufficiently broad size distribution. We used a scanning mobility particle sizer and an aerodynamic particle sizer to determine particle number and size. The set-up was used to investigate individual differences in the deposition fraction (DF) of particles in the respiratory tract for a group of 67 subjects of both sexes aged 7–70 years. The measured DF was applied to two model aerosols, one representing an urban environment and one a rural environment, and the particle deposition rates were derived (i.e., the deposited amount of particles per unit time). Furthermore, the deposition rates were normalized to lung surface area and body mass – two dose measures that are considered relevant for the health effects of airborne particles. In addition to validation of the set-up, we show that there is a large individual variation in DF, with some subjects having a DF that is more than twice as high as that of others. Although we observe differences in the DF between different subgroups, most individual variation was explained neither by age nor by gender. When normalizing the deposition rates to lung surface area or body mass, the deposition rates of children become significantly higher than those of adults. Furthermore, the individual variability is larger for the lung surface area or body mass normalized deposition rates than for DF.

Keywords: Aerosols; Airborne particles; Deposition efficiency; Individual variability; Dose rate.

INTRODUCTION

In order to understand the health effects of inhaled air pollution particles it is necessary to determine the dose deposited, here defined as the amount of particulate material that deposits in the respiratory tract during exposure. The dose is governed by a number of factors including particle concentration, exposure time, breathing pattern, ventilation rate, lung morphology and characteristics of the particles such as size, hygroscopicity, shape and density (ICRP, 1994). The least known of these factors are usually those related to the exposed individuals: breathing behavior and intrinsic properties of the respiratory tract.

Substantial efforts have been made, both theoretically and experimentally, to assess the respiratory tract deposition of aerosols. Model calculations generally have the advantage of being able to estimate deposition probabilities in different regions of the lungs, but are unable to replicate the full complexity in flow fields, in geometry of the airways, and in dynamic changes in lung morphology or individual variability. Furthermore, models are usually limited to healthy adults. Experimental data are thus necessary for validation of the models and to assess the dose.

Most measurements of the deposition of inhaled particles have been carried out on healthy (male) adults, but some also include children (Becquemin *et al.*, 1991; Schiller *et al.*, 1992; Schiller-Scotland *et al.*, 1994; Bennett and Zeman, 1998; Smith *et al.*, 2001; Bennett and Zeman, 2004; Isaacs and Martonen, 2005; Olvera *et al.*, 2012), elderly people (Kim *et al.*, 1988; Bennett *et al.*, 1996; Kim and Jaques, 2005),

* Corresponding author.
Tel.: +46 70 151 84 26
E-mail address: jenny.rissler@sp.se

and patients with airway diseases (e.g., Kim *et al.*, 1988; Schiller-Scotland *et al.*, 1996; Bennett *et al.*, 1997; Brown *et al.*, 2002; Chalupa *et al.*, 2004; Möller *et al.*, 2008; Löndahl *et al.*, 2012). The studies are not fully conclusive, but several of them report an increased respiratory tract deposition for patients with lung diseases and for children. A limitation of all these studies is that they include a small number of monodisperse particle sizes, or narrow size ranges of polydisperse aerosols. For instance, no experimental data at all are available for children or elderly people for particles between 200 and 1000 nm, although this is a size range that often contains a large mass fraction of ambient aerosols. Thus, deposition and dose information is sorely needed, especially for vulnerable subgroups for which the knowledge can be of use also in tailoring aerosol drug delivery.

Little research has been carried out to develop methodology that can cover a broad size interval of fine and ultrafine particles, and the existing systems have only been used for a few healthy subjects, almost all of which are adult males (van Wijk and Patterson, 1940; Landahl and Herrmann, 1948; Dautrebande *et al.*, 1959; Heyder *et al.*, 1975; Rosati *et al.*, 2002; Montoya *et al.*, 2004). Since there is no common standard in methodology, results are generally difficult to compare. Hence, there is a need both for experimental techniques that can measure the respiratory tract deposition of polydisperse aerosols over a wide size range, and for data obtained with a similar methodology for a larger group of people of different ages.

The objective of this study is to develop an experimental set-up, and use this to investigate the individual variability in respiratory tract deposition of airborne particles for: (*i*) a large group of subjects (67) of different ages (7–70 years) and gender, and (*ii*) for most of the respirable aerosol particle size fractions (15–5000 nm). We also analyze the individual variation in the measured deposition fractions (DFs) and discuss implications of the data for real-world exposure situations. This is, to our knowledge, the most extensive data set collected of its kind.

METHODS

Study Design

Particle deposition efficiency was determined in a sample of 67 non-smoking subjects aged 7–70 years, (39 female and 28 male), whereof 7 were aged 7–12 years. Individuals between 12 and 20 years of age were not included due to the rapid development of the lungs, with high intra-individual variability, occurring sometime in this age window. Each participant went through a comprehensive lung function investigation, performed on a separate day. The study was approved by the regional ethics committee in accordance with the Declaration of Helsinki. The participants were given both oral and written information and they provided their written consent before the study began.

SPSS (IBM©SPSS© Statistics, v 23) was used for the statistical analysis. The correlation analysis was calculated with Pearson's product moment and significances of differences between groups were calculated with the Student's t-test and the Mann-Whitney U-test. The significances considered were those at the 0.05 or 0.01 levels.

The RESPI$_2$ Set-up

The set-up used for the respiratory tract deposition measurements was an improved version of a set-up described in several previous publications (e.g., Löndahl *et al.*, 2006; Rissler *et al.*, 2012), and followed the general experimental guidelines described in Löndahl *et al.* (2014). The new set-up is referred to as RESPI$_2$.

The main improvement of the RESPI$_2$, compared to the original RESPI, was extension of the particle size interval to include diameters from 15 nm to 5 μm. Previously, the upper size limit of the set-up was 500 nm. In short, this was achieved by:

1) Introducing a second instrument flow line and associated valves.
2) Introducing a second analyzing instrument, the APS (Aerodynamic Particle Sizer), which detects particles of aerodynamic diameters from around 0.5 μm up to 20 μm.
3) Redesigning the system to minimize losses of the larger particles (tilting the exhalation tank, selecting valves with low particle losses due to impaction, and optimizing the flow lines).
4) Software development for controlling the new set-up and logging of data.

Similar to the previous version, the RESPI$_2$ set-up was based on a continuous flow-through of the aerosol without stagnant collection in bags. The size-dependent deposition fraction (DF) was determined by comparing the particle number size distributions in the inhaled and exhaled air. The instruments used for the size characterization were a Scanning Mobility Particle Sizer, SMPS, (design: Lund University, Löndahl *et al.* (2006)), and an APS (model 3321, TSI®). A computer program (written in LabVIEW 8.2) was developed to control the valves and the SMPS, record the size distributions, log inhalation and exhalation flows, and to log temperatures and relative humidity (RH) at several positions in the flow lines.

Aerosol samples of 0.95 L min^{-1} were alternatingly led from the inhalation and exhalation tanks to the SMPS and the APS, as illustrated in Fig. 1. In order to achieve similar particle losses during transportation from each tank to the respective characterization instruments, the paths of the aerosols from each tank were designed to be as similar as possible (illustrated in Fig. 1 and Fig. S1). To minimize electrostatic particle losses, all flow lines were made of electrically conducting material, including the duckbill valves (silicon rubber coated with a 50 nm thick layer of gold [Löndahl *et al.*, 2006]). To achieve low losses, 3-way ball valves were used (Swagelok® model MS-142DCXE, 24 V DC). In the previous version, the RESPI tanks were placed horizontally at an angle of 90° to one another. To further decrease losses due to sedimentation in the system, the exhalation tank was tilted downwards in a 45° angle relative to the horizontal plane. More details about the SMPS are found in the Supplemental Material (SM).

The flow-dependent particle losses of the system as a whole were determined prior to the experiments and

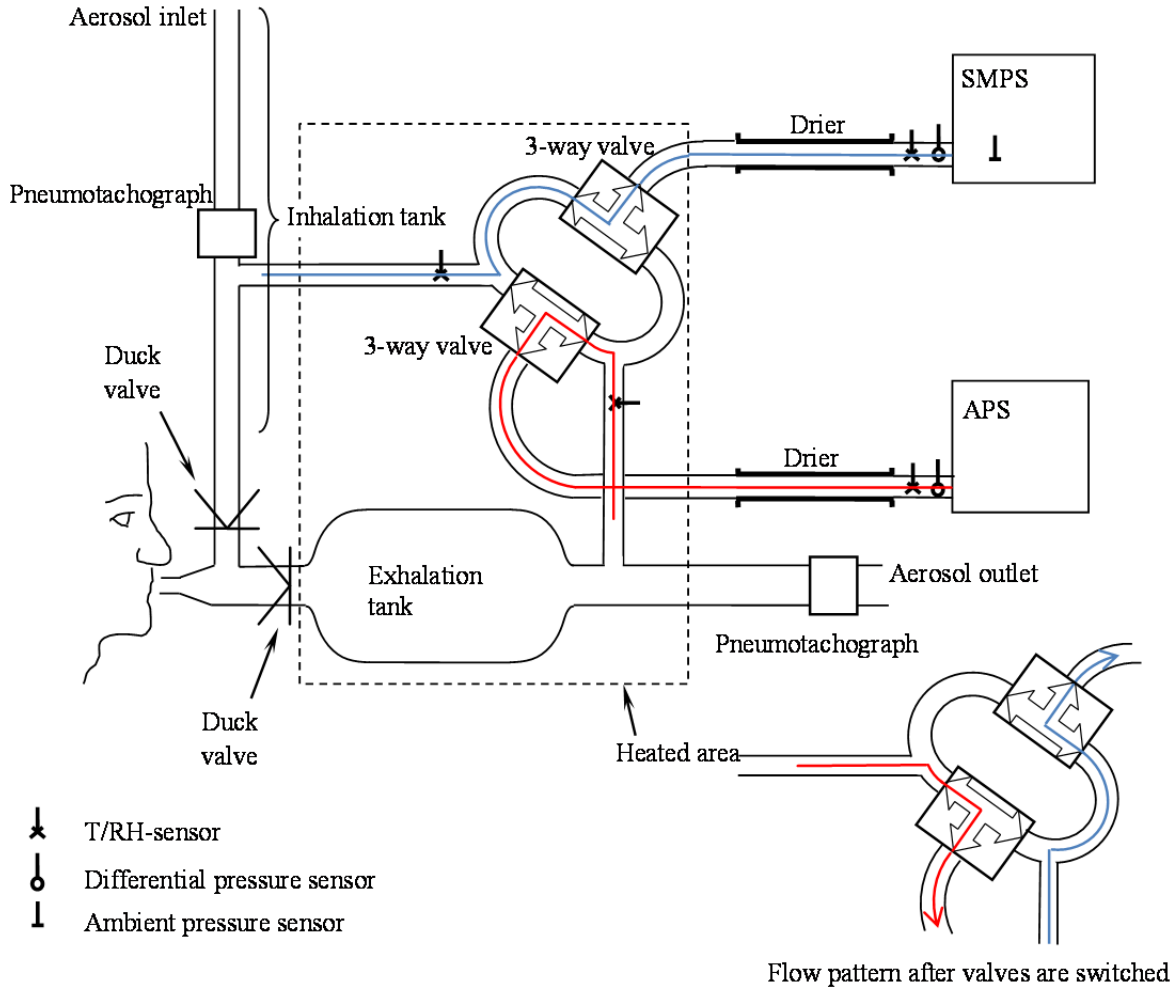

Fig. 1. A schematic picture of the $RESPI_2$ set-up. Arrows indicate the flows, where the red arrow represents the APS flow and the blue arrow the SMPS flow. The flows after switching the valves are shown in the lower right corner of the main figure.

compensated for as described in Löndahl *et al.* (2006). The particle losses were determined using the same particles as during the lung deposition measurements (carnauba wax and glass spheres). An example of typical size-dependent system losses is shown in Fig. S2. The characterization of instrumental losses was performed in an interval from 2 to 20 L min^{-1} and performed at constant flow (because the deposition by diffusion and sedimentation is governed by the total residence time and not air velocity). Initially the instrumental losses were tested using a sinus wave piston-type breath simulator connected to the inlet of the breathing system, as described in Löndahl *et al.* (2006). No apparent differences were observed compared to using a constant flow. Apart from instrumental losses, a correction to DF was also made due to mouthpiece dead space. The container for exhaled air was heated to approximately 37°C to avoid condensation of water vapor, and the aerosol was dried to a relative humidity < 20% before entering the SMPS and the APS.

In the set-up, the SMPS characterized the particle number size distribution in the diameter size range of 15 to 500 nm. An SMPS classifies the particles according to their mobility diameter, d_{me} (identical to the thermodynamic diameter). The mobility diameter is related to the diffusivity of the particles and has been proven to be the equivalent diameter that best describes the lung deposition for particles < 300 nm), regardless of particle shape or density (Heyder *et al.*, 1986; Schmid *et al.*, 2008; Rissler *et al.*, 2012). Deposition by diffusion is governed by the particle diffusivity, D, which is related to mobility diameter as $1/d_{me}$.

The APS classifies particles according their equivalent aerodynamic diameter (d_{ae}). In this study, the density correction to account for being outside the Stokes regime was applied according to the procedure of the APS software. In the $RESPI_2$, the APS covered the diameter size range from 0.8 µm up to 5 µm. The lower size limit was constrained by the low counting efficiency of the APS for particles with diameters below about 0.8 µm and the upper size limit by the particle losses in the $RESPI_2$. The equivalent aerodynamic diameter is expected to be the relevant size measure that determines the lung deposition of particles > 500 nm, regardless of mass, volume, shape or density of the particles. The two main deposition mechanisms in this size interval are gravitational settling (sedimentation) and inertial impaction.

Due to the above mentioned, the diameters presented in Figs. 2 and 6 are mobility diameters in the size range of the SMPS, and aerodynamic diameters in the size range of the APS. This is also the way the data should be applied – for particle mobility size in the small diameter range and for particle aerodynamic size for the larger particles. For spherical particles, the mobility diameter is identical to the volume equivalent diameter (and the geometrical diameter), which is also true for the aerodynamic diameter when particles are spheres of unit density.

Lung Deposition Measurement Procedure

The size-dependent particle deposition fraction in respiratory tract was measured during spontaneous oral breathing while sitting. A nose clip was used. After a short test period, during which the subject became familiarized with the equipment, the deposition pattern was measured during two periods of 12 minutes each. The DMA scan time was set to 90 seconds (up-scans and down-scan were 90 s each). To ensure complete mixing in the lungs and in the instrument, the first minute of the measurement was discarded. The breathing pattern was recorded using two pneumotachographs placed in the inhalation flow and exhalation flow. The pneumotachographs were calibrated regularly throughout the experiments. The recorded flow was converted into BTPS (body temperature and pressure, saturated) based on the continuous measurements of temperature (T) and relative humidity (RH) in the system (Fig. 1). The tidal volume referred to hereafter is that which was recorded during the RESPI measurements.

Aerosol Generation

Hydrophobic particles were used to avoid particle size changes due to water uptake at the high relative humidity in the lung (99.5%). The particles were of two types (i) carnauba wax particles of a distribution covering the size range 15–500 nm, and (ii) manufactured glass particles in a size range of 0.5–5 μm. The carnauba wax particles were generated by an evaporation-condensation process and the glass particles were dispersed into air by a Vilnius Aerosol Generator (VAG, CH Technologies, Inc., Westwood, NJ). A stable aerosol was generated in a large mixing chamber (22 m^3 stainless steel chamber) with a controlled RH (45%), temperature (21°C) and air exchange rate (1 h^{-1}), to which the inhalation tank was connected. To avoid evaporation-condensation or particle restructuring in the lungs, the particles were heated before entering the inhalation tank (see Fig. S4). More details of the particle generation and size distributions are provided in the SM (Section S4).

Lung Function Test

Each subject went through a comprehensive lung function investigation. An overview of the subjects' demographics and lung function is given in Table 1. The breathing variables recoded during the deposition measurements are also presented. The relationship between lung function and particle deposition is investigated in more detail in a separate study (Rissler *et al.*, 2017).

Table 1. Subject demographics, lung function and breathing parameters (at BTPS) during particle deposition experiments. V_T is tidal volume, T_{bc} the time of a breath cycle, VC Vital Capacity, and FEV1 Forced Expiratory Volume in 1 second.

Age (year)	Males	Females	Height (cm)	Weight (kg)	V_T (L)	T_{bc} (min)	VC (L)	VC (% of pred)	FEV_1 (L)	FEV_1 (% of pred)
7–12 (Children)	7		142 (± 14)	40 (± 13)	0.51 (± 0.13)	0.063 (± 0.011)	2.4 (± 0.6)	103 (± 9)	1.9 (± 0.6)	95 (± 17)
20–29	6	13	170 (± 8)	64 (± 12)	0.73 (± 0.22)	0.100 (± 0.042)	4.5 (± 0.6)	105 (± 8)	3.9 (± 0.6)	104 (± 9)
30–39	6	7	177 (± 11)	73 (± 13)	0.77 (± 0.29)	0.102 (± 0.035)	5.0 (± 1.3)	110 (± 8)	4.1 (± 1.1)	107 (± 11)
40–49	3	3	174 (± 8)	73 (± 13)	0.71 (± 0.18)	0.085 (± 0.023)	4.7 (± 0.7)	114 (± 13)	3.7 (± 0.6)	108 (± 7)
50–59	5	7	173 (± 8)	82 (± 13)	0.79 (± 0.22)	0.104 (± 0.035)	4.1 (± 0.9)	109 (± 13)	3.2 (± 0.5)	104 (± 12)
60–70	5	5	171 (± 8)	79 (± 11)	0.73 (± 0.14)	0.103 (± 0.019)	3.7 (± 0.9)	107 (± 18)	2.8 (± 0.7)	101 (± 17)
Av. adults	25	35	173 (± 9)	73 (± 14)	0.75 (± 0.22)	0.100 (± 0.034)	4.4 (± 1.0)	108 (± 12)	3.6 (± 0.9)	105 (± 11)

Analyzing the Lung Deposition Patterns

The measured size-resolved lung deposition fraction (15–5000 nm) was described by the equation:

$$Df\left(d_p\right) = A_k + B_k d_p - C_k d_p^2 - \frac{1}{D_k\left(C_c / d_p\right)^{E_k}} \quad (1)$$

where A_k, B_k, C_k, D_k, and E_k are constants, d_p is the measured particle diameter, and C_c is the Cunningham correction term (Hinds, 1999). Eq. (1) was based on Rissler *et al.* (2012), with minor modifications. The equation was fitted to the DF(d_p) curves of each subject by using a least square approach. The fitted individual curves were used for calculating the particle deposition rates in the respiratory tract (described in the next section). This was because the fitted curves were continuous while the measurements did not cover the interval 500–800 nm. The equation was also fitted for the average lung deposition pattern of the population divided into adults and children.

To achieve better statistical power in the analysis of the differences between subpopulations, the measured deposition fractions were pooled in ten logarithmic size bins: 15–30 nm, 30–50 nm, 50–100 nm, 100–200 nm, 200–350 nm, 850–1300 nm, 1300–1900 nm, 1900–2700 nm, 2700–3500 nm, and 3500–5000 nm.

Dose Estimates for Model Aerosols

In order to estimate the total deposited fraction (TDF) and the deposition rate (Drate), which is the deposited dose per time unit, the measured DF(d_p) must be applied to aerosols of specific size distributions. For the purpose of illustrating the effect of individual variability in DF on TDF and Drate, we applied the measured DF to two model aerosols. The model aerosols had particle size distributions identical to those found at: (i) a busy street in central Copenhagen, Denmark (referred to as Model Aerosol 1), and (ii) a rural site in Scania, in southern Sweden (referred to as Model Aerosol 2), see Rissler *et al.* (2014). The aerosol found at the busy street was dominated, at least with respect to number, by ultrafine or nano particles. The number size distribution was described by two log-normal functions peaking at 10 and 52 nm (GMD_1: 10 nm, σ_{g1}: 2.2 , N_{F1}: 0.57, GMD_2: 52 nm, σ_{g2}: 2.4, N_{F2}: 0.43, where GMD is the particle geometric mean diameter, σ_g is the geometric standard deviation and N_F is the number fraction in each mode). At the rural site, the aerosol number size distribution was described by two log-normal functions peaking at 87 and 179 nm (GMD_1: 87 nm, σ_{g1}: 1.5, N_{F1}: 0.65, GMD_2: 179 nm, σ_{g2}: 1.3, N_{F2}: 0.35). When converted to particle volume (or mass) size distributions, the particles found at the busy street were described by a unimodal size distribution with a GMD of 620 nm (σ_g: 2.6) and the rural site particles by a distribution with a GMD of 304 nm (σ_g: 1.6). More information about the aerosols can be found in Rissler *et al.* (2014).

The estimations of TDF and Drate were carried out only to provide examples of how the individual variation in DF results in an individual variation in dose. The calculations were not made in great detail. For example, we used the assumption that the particles were hydrophobic and spherical in the calculations. Particle hygroscopicity is known to alter the particle size in the lungs, and thus alter DF (Morrow, 1986; Löndahl *et al.*, 2007). For particles < 400 nm, particle shape has no effect on DF if one is referring to the number of particles as a function of equivalent mobility particle diameters (Rissler *et al.*, 2012), as measured by the SMPS. However, for fractal-like particles, with a size-dependent effective density, the peak in mass size distribution is slightly shifted compared to particles of a non-size-dependent density (Wierzbicka *et al.*, 2014), and may thus alter both the TDF and the Drate. The absolute density of the particles should not affect TDF or Drate by particle number if predicted from the mobility diameters in the size range where diffusion is the main particle deposition mechanism, and the aerodynamic diameters in the size range where sedimentation and impaction are the dominant deposition mechanisms.

RESULTS AND DISCUSSION

Lung Deposition Fraction

The measured lung deposition fraction, DF(d_p), followed the expected pattern with a minimum in the 300–500 nm diameter size range (Fig. 2(a)). To show the individual variability in the DF, boxplots of the size-binned data are shown in Fig. 2(b). Furthermore, all individual DF(d_p) curves are shown in SM (Fig. S3). The complete set of measured DFs together with lung function is published elsewhere (Rissler *et al.*, 2017). The average DF of the children was higher than that of the adults by 11%, but the difference was not statistically significant ($p = 0.21$). The curves fitted to the average deposition fraction of the adults and children (Eq. (1)) are also shown in Fig. 2(a), and the fitted parameters are presented in Table 2.

For particles of diameters < 3500 nm, individuals with a high deposition of a certain particle size had a high deposition for all particles. In this size range, the Pearson's correlation coefficients between a DF of one size fraction, paired with DFs of other size fractions for the same individual, were 0.8–0.9. Thus, it appeared that despite the fact that the deposition of particles < 500 nm and particles > 500 nm typically is governed by different mechanisms (diffusion for the smallest and sedimentation or impaction for the larger) the variables controlling the individual DFs affected the deposition in the two regimes similarly. This is consistent with that deposition by both diffusion and sedimentation increase with increasing residence times and decreasing tube dimensions. When pairing DFs of particles > 3500 nm with those of particles < 3500 nm, there was a clear drop in correlation that decreased with increasing size. The mechanisms by which deposition occurred seemed to be altered for particles > 3500 nm, probably explained by deposition by impaction in the upper airways coming into account for the largest particles. We did see a similar trend in the data set for children, but not as large. This is further elaborated in the study focused on the correlations between DF and lung function (Rissler *et al.*, 2017).

The difference observed in DF between men and women was minor and not significant (6% higher DF for the females,

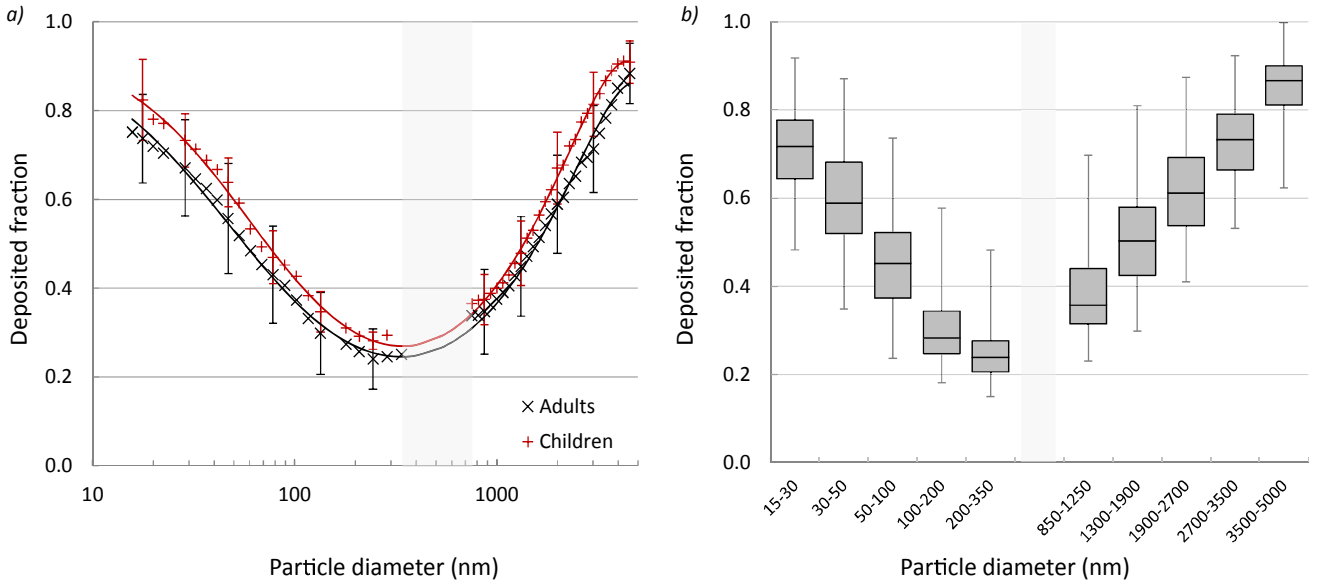

Fig. 2. (a) shows the average lung deposition curves of adults (black markers) and children (red markers), together with the corresponding fitted functions (solid lines). The error bars correspond to one standard deviation of the individual variation in deposition fraction. In (b), the data are binned into logarithmic size bins and presented as boxplots where the boxes represent the median, and the 1st and 3rd quartiles, and the bars the minimal and maximal DFs observed. The data include adults only.

Table 2. Parameters describing the average particle deposition in the interval 15–5000 nm for children and adults when inserted into Eq. (1).

	Ak	*Bk*	*Ck*	*Dk*	*Ek*
Adults	0.960	0.356	0.191	0.087	0.584
Children	0.952	0.414	0.215	0.085	0.644

p = 0.13). There was also a non-significant decrease in DFs with age observed when comparing the groups of ages 7–12 y, 20–30 y and 30–70 y (the DF for children was 3% higher than for 20–30 y, while DF for the oldest group was on average 6% lower than that of subjects of ages 20–30 y). Neither was any statistically significant correlation observed between age and DF from the bivariate analysis of the adult group, even if other lung variables, such as FEV1 and RV, did correlate with age.

In two earlier studies, the DF of children and adults were studied and compared (Schiller-Scotland *et al.*, 1994; Bennett and Zeman, 1998). In the Schiller-Scotland *et al.* (1994) study, the measured DF of the children was 50% higher compared to the adults, while Bennett and Zeman did not observe any significant differences in DF between children and adults. In the study by Bennett and Zeman (1998), controlled relaxed breathing was used while Schiller-Scotland *et al.* (1994) used spontaneous relaxed breathing. Bennett and Zeman (1998) explained the large difference observed between the two groups by Schiller-Scotland *et al.* (1994) as an effect of the mouthpiece, resulting in the children increasing their tidal volume compared to normal relaxed breathing. The set-up in our study was similar to that of Schiller-Scotland *et al.* (1994) in the sense that our experiments were performed during spontaneous relaxed breathing through a mouthpiece. However, we saw only a minor (3%), non-significant, difference between children and young adults (the young adults in this study matches the ages of the adults in the Schiller-Scotland *et al.* [1994] study). One explanation may be that the mouthpiece dead space in our study was relatively small (31 mL), another may be that our system had a different air-flow resistance. The DFs reported here were higher than those reported in the study by Bennett *et al.* (1998) and comparable to those in Schiller-Scotland *et al.* (1994).

We saw some trends in the DF between different subpopulations, but the differences between the groups were minor compared to the variation between individuals within a group. The data showed that some subjects may have DFs that are more than twice as high as for others. This observation has also been reported in other studies (Löndahl *et al.*, 2007).

Comparison of DF with Previous Findings

The deposition pattern reported in this study was in principal similar to that found previously in both experiments and by model calculations. To put our data in perspective, our DF(d_p) curve was compared to that modelled using three deposition models. The deposition models used were ICRP (ICRP, 1994), MPPD (Anjilvel and Asgharian, 1995) with lung geometry and airway dimensions from Yeh & Schum whole lung (Yeh and Schum, 1980), and NCRP (Cuddihy *et al.*, 1997) with a lung structure and airway dimensions from either the Weibel A model (Weibel, 1963) or Yeh & Schum whole lung (Yeh and Schum, 1980), as modified by Yu and Diu (1982). The average tidal volume (V_T), the time of one breath cycle (T_{bc}) and functional residual capacity (FRC) of the adult group was used as input to the model, see Table 1 and Rissler *et al.* (2017). The results are shown

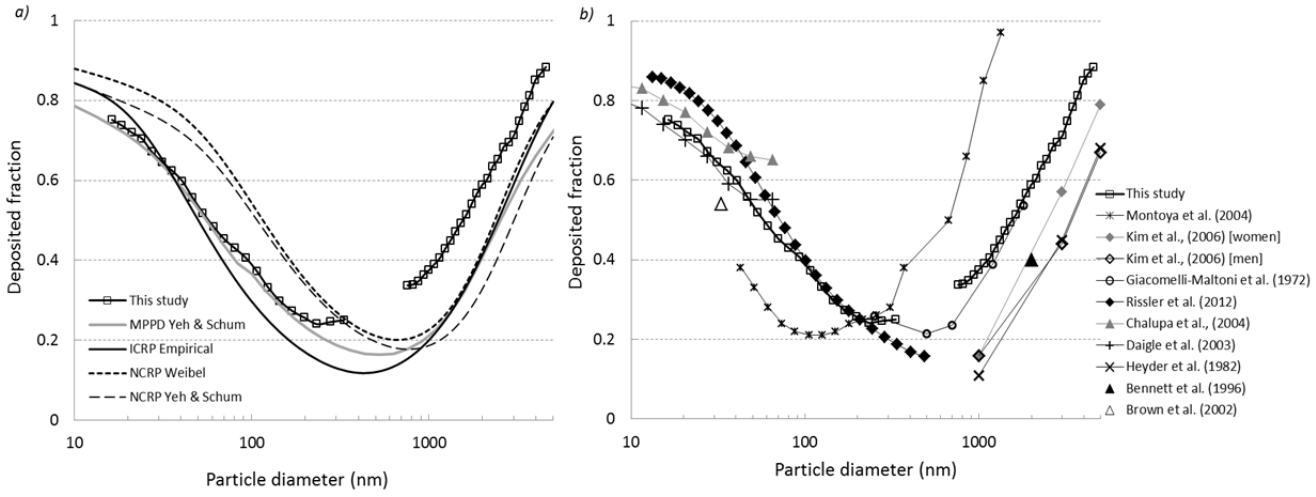

Fig. 3. DF curves of this study compared to (*a*) modelled DFs and (*b*) previously reported experimental DFs. In (*a*), the models included were i) the MPPD model (Anjilvel and Asgharian, 1995) using the whole lung model of Yeh & Schum (Yeh and Schum, 1980), ii) ICRP model (ICRP, 1994), and iii) and iv) the NCRP model (Cuddihy *et al.*, 1997) with a lung structure and airway dimensions from either the Weibel A model (Weibel, 1963) or Yeh & Schum whole lung (Yeh and Schum, 1980), as modified by Yu and Diu (1982). The models were applied using a functional residual capacity (FRC) of 3400 mL, a tidal volume (V_T) of 750 mL, and the time of one breath cycle (T_{bc}) of 0.10 min (or 10 breaths/minute). These values correspond to the averages for the adult group in this study. The experimental studies referred to in (*b*) are Montoya *et al.* (2004), Kim *et al.* (2006), Giacomelli-Maltoni *et al.* (1972), Rissler *et al.* (2012), Chalupa *et al.* (2004), Daigle *et al.* (2003), Heyder *et al.* (1982), Bennett *et al.* (1996), and Brown *et al.* (2002). When data for different breathing patterns were available, the data with the breathing patterns closest to that in the present study was used (Kim *et al.*, 2006). From the study by Giacomelli-maltoni *et al.* (1972) data for mouth breathing was used. Note that subjects in the study by Chalupa *et al.* (2004) were asthmatic.

in Fig. 3(a) together with the measured average DF(d_p) curve. For small particles (smaller than the minima in DF ~400 nm) the modelled data varied considerably: for 100 nm particles DF ranged from 0.32 to 0.57. In this study we found a DF of 0.38. For the large particles (larger than the minima in DF) our measured DFs were higher than those modelled. For 2 μm particles the models estimated DFs that ranged between 0.35 and 0.45, while our measurements show a DF of 0.6. It is unclear if this discrepancy is due to limitations of the models or an unidentified systematic bias of the experimental data.

There are no previous experimental studies that cover the full size range of 15–5000 nm, and very few that cover particles on both sides of the minima in the deposition curve. For particles below the minima, where diffusion is the dominating deposition mechanism, there is good agreement between the DFs here reported and those found in previous studies on healthy subjects, during spontaneous breathing of hydrophobic particles (Heyder *et al.*, 1982; Bennett *et al.*, 1996; Daigle *et al.*, 2003; Chalupa *et al.*, 2004; Wiebert *et al.*, 2006a, b; Löndahl *et al.*, 2007; Löndahl *et al.*, 2012; Rissler *et al.*, 2012), as shown in Fig. 3(b). For particles above the minima the experimental data are more diverse. We report DFs that are 0.2–0.3 higher than those found by Heyder *et al.* (1982) and Bennett *et al.* (1996), but lower than those found by Montoya *et al.* (2004), and in a similar range as some (Giacomelli-Maltoni *et al.*, 1972; Chan and Lippmann, 1980; Melandri *et al.*, 1983). The measured DFs were not fully intercomparable since the breathing patterns and lung physiology of the subjects differed, but the differences in the observed DFs were larger than expected from that.

Applied to Model Aerosols

In an attempt to illustrate the individual variation in the total deposited fraction (TDF) and deposition rates (i.e., the deposited amount of particles per unit time), the measured deposition fraction for each subject was applied to model aerosols, based on ambient particle size distributions. For this purpose, the fitted deposition efficiency curves were used in order to obtain a continuous function. The TDF was determined by particle number (TDF_N) and by particle mass (TDF_M). Another relevant dose metric is particle surface area (Schmid and Stoeger, 2016). The TDF of the particle surface area should lie between TDF_N and TDF_M, and with a similar individual variation. For the estimations, two hydrophobic model aerosols were used: Model Aerosol 1 (MA1), with a size distribution similar to that found at a busy street and Model Aerosol 2 (MA2), with a distribution similar to that found at a rural site. The calculations were performed for each subject individually.

The resulting TDFs of the four distributions (number and mass concentrations for MA1 and MA2) are presented as boxplots in Fig. 4 and in Table 3. The change in TDF with aerosol type was mainly determined by the GMD and σ_g of the particle size distributions (mass size distributions were altered relative to number size distribution towards larger sizes). The closer the GMD of the particles was to the

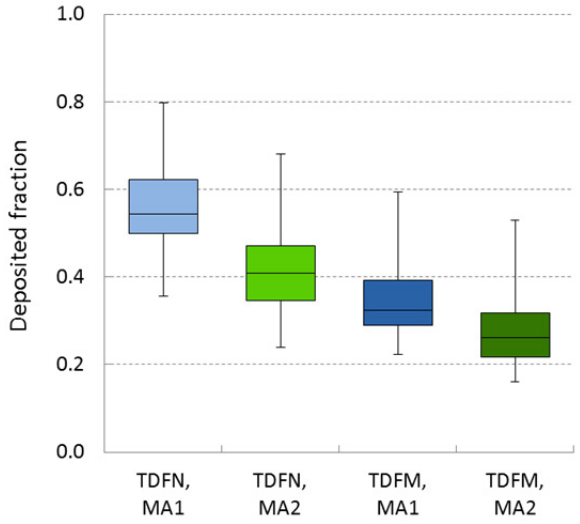

Fig. 4. The Total Deposited Fraction (TDF) in the lungs when exposed to two model aerosols: Model Aerosol 1, MA1 (a hydrophobic aerosol with a size distribution similar to that found at a busy street), and Model Aerosol 2, MA2 (a hydrophobic aerosol with a size distribution similar to that found at a rural site). TDFs were determined both for the number concentrations (indexed N) and mass (M). The boxes represent the median, and the 1st and 3rd quartiles, and the bars the minimal and maximal TDFs. The data include adults only.

Table 3. The median TDF found for two model aerosols. To quantify the individual variability, the quartiles Q1 and Q3 are given, as well as the minimum and maximal TDFs, for MA1.

	TDF_N		TDF_M	
	Adults	Children	Adults	Children
TDF (MA1)	54%	61%	32%	35%
Min	*36%*	*57%*	22%	34%
Q1	*50%*	*60%*	29%	35%
Q3	*62%*	*62%*	39%	39%
Max	*80%*	*73%*	59%	47%
TDF (MA2)	41%	45%	26%	28%

minimum in the DF(d_p) curve (Fig. 2), the lower the TDF. Note that the GMD for the mass size distribution of MA1 was actually larger than the size at the minimum in the DF curves. The individual variation in DF was passed on to TDF and thus, the observed differences in TDF between adults and children were not significant ($p > 0.05$). As for DF, the individual variation in TDF within the group of children was not as pronounced as within the group of adults.

Another, and perhaps even more relevant, measure for estimating the dose to the lungs is the deposition rate (Drate). Drate includes the effect of the minute volume ventilation (V_E) of the individuals. The average Drate for the male subjects was slightly higher than for the females (by 7%), but the difference was not statistically significant ($p = 0.21$). The Drate for children was typically 20% higher than that of the whole group of adults, both when referring to particle number and mass, a difference that was statistically significant ($p < 0.05$). The fact that the difference in Drate of children compared to adults was larger than that in DF or TDF is explained by the higher breathing frequencies of the children, leading to higher minute ventilation rates despite their typically smaller tidal volumes. An additional dose measure that is relevant for the health effects of airborne particles is the deposition rate normalized to either lung surface area ($nDrate_{LSA}$) or body mass ($nDrate_{BM}$). The lung surface area was, for the purpose, estimated as the lung volume (FRC) to the two-thirds power, as described in Bennett and Zeman (1998). The deposition rates (normalized and not normalized) were estimated for all four distributions, whereof the boxplot in Fig. 5 illustrate the deposition and inter subject variability of MA1 (the city aerosol), with respect to particle mass, for adults and children. The inter-subject variability was similar for all four aerosol distributions. In the plot, all values are normalized to the corresponding median deposition rate of the adult group.

As for DF and TDF, the individual variation of the children in Drate was less than for the adults. However, when normalized to lung surface area or body mass, the variation became much larger than for the adult group. Furthermore, the normalized Drates ($nDrate_{LSA}$ and $nDrate_{BM}$) of the children were significantly higher than those of the adults with an average nDrate more than twice that of the adults, as illustrated in Fig. 5. Looking at the whole group of subjects (both adults and children) a statistically significant trend of decreasing $Drate_{BM}$ with age was observed, probably explained by the increase in weight with age. No similar trend was observed when normalizing the dose to lung surface area, except that children as a group had a higher $nDrate_{LSA}$ than the adults. The average nDrate of the female subjects was higher than that of the male subjects, both when normalizing lung surface area and body mass, by around 10–15%. The difference in nDrate between the two groups was statistically significant only when normalizing it to body mass ($p < 0.05$).

Measurement Uncertainties

There are many critical aspects to consider when performing measurements of respiratory tract particle deposition. Löndahl *et al.* (2014) reviewed these and discussed their influence on experimental findings (summarized in Table 1 in that study). Examples of critical aspects are unstable particle concentration, electrostatic particles, pressure variations, condensation of water, monitoring respiratory flows, assuring accurate size determination, and that the proper equivalent particle diameter is determined. The factors listed by Löndahl *et al.* (2014) that are related to the system design, such as pressure variations or instrumental losses, were considered during the design of the $RESPI_2$.

The uncertainty in particle size of the DF(d_p) curve was set by the uncertainty of both detection instruments and calibration procedures. In this study, the accuracy of the size determination was checked through calibration with standards of monodisperse polystyrene spheres of 100 nm (for the SMPS) and 5 µm (for the APS). Since DF is the relative difference between inhaled and exhaled concentrations, the required accuracy in absolute concentration is of minor

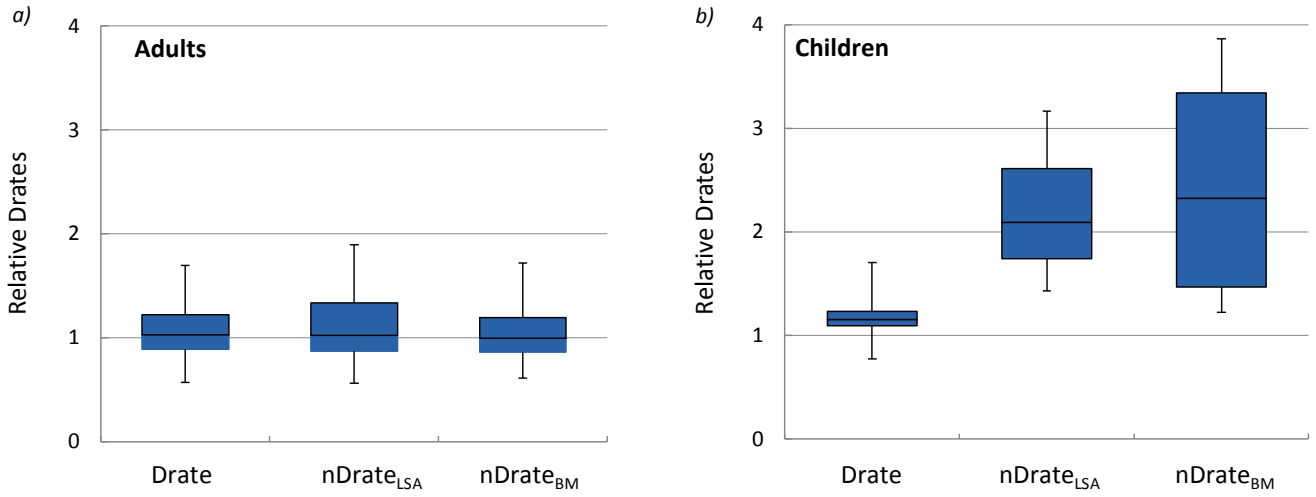

Fig. 5. The deposition rates (deposited dose per time unit) for the mass size distribution of Model Aerosol 1, as well as Drates normalized to lung surface area ($nDrate_{LSA}$) and subject body mass ($nDrate_{BM}$). All values are normalized to the median deposition rates of the adult group. The boxes represent the median, and the 1st and 3rd quartiles, and the bars the minimal and maximal values.

importance as long as the measurement precision is high and linearly related to the concentrations.

All spectra (90 s time resolution) were checked to identify any variations in concentration over time, and if identified, the measurements were excluded from the analysis. In an attempt to estimate the uncertainties related to the accepted variations in aerosol number concentration and size, the 95% two-sided confidence intervals were estimated (97.5th percentiles of the t-distribution) for the DF(d_p) curve of each individual. These calculations were based on the variation in the aerosol number size distribution during the measurement of the DF curve for each subject. The standard deviation of the DF for each subject was achieved from deposition curves calculated from each size scan and the average of its two neighboring scans. From the standard deviation, the confidential intervals for the deposition curve of each subject were estimated. The average and median confidence intervals for the individual DF curves are presented in Fig. 6. Note that this is the average uncertainty of all individual DF(d_p) curves and not the uncertainty in the DF average curve (shown in Fig. 2), which is smaller. As reflected by the graph in Fig. 6, the variation in the distributions resulted in the largest uncertainty on the steep gradients of the size distributions.

In this study, as for all studies using a polydisperse aerosol, one critical issue was particle size shifts. Systematic size shifts after inhalation, due to particle restructuring or particle evaporation, introduced the largest uncertainty in the DF(d_p) curve. A size shift occurring between sizing of inhaled and exhaled particles will lead to erroneous interpretation of the size-resolved particle deposition fraction, as also discussed in the paper by Löndahl *et al.* (2014), and illustrated in their Fig. 8. The effect of this is further discussed in the SM and illustrated in Fig. S6. For broad unimodal distributions, particle size shifts are often masked and are not obvious from looking at the deposition curve. In this study, due to the three distinct peaks in the sub-micrometer size distribution, any shift in the distribution became evident in the derived deposition pattern since that resulted in a wobbling of the DF curve, as demonstrated in Fig. S6. As illustrated, even a small size shift resulted in uncertainties in the measured DF. There were obvious problems with size shifts in the pre-study. To avoid this, a heater was introduced before the particles entered the inhalation tank of the $RESPI_2$ (Fig. S4), however, for the sub-micron particles in this study it was nearly impossible to get rid of any effect of this – which may have resulted in a slight underestimation of the DF in the very small size range, and a slight overestimation of the DF in the minima (compare to Fig. S6). However, the shape of the DF curves did correspond to those typically modelled, even if the DF curve was partly shifted compared to the modelled one. This shift cannot be explained solely by any particle size shift.

SUMMARY AND CONCLUSIONS

The exposure of airborne particulates may pose different health risks to different individuals and subpopulations. One important factor in understanding the individual differences in response to air pollution is the variation in the lung deposited fraction of particles. Thus, when a population is exposed to similar air pollution levels, the dose deposited in the lungs can differ significantly between individuals. Understanding the individual variability in lung deposition can also be used for tailored aerosol drug delivery.

In this study we describe an experimental set-up for measurements of lung deposition of particles covering the full size range of 15 to 5000 nm and the resulting size-dependent deposition fraction of the 67 subjects, aged 7 to 70 years. The set-up enables us to compare the DF of different particle size fractions covering nearly the full inhalable particle size fraction, from 15 to 5000 nm. This size range covers particles that are deposited with different mechanisms and in different parts of the lungs. As an example, data

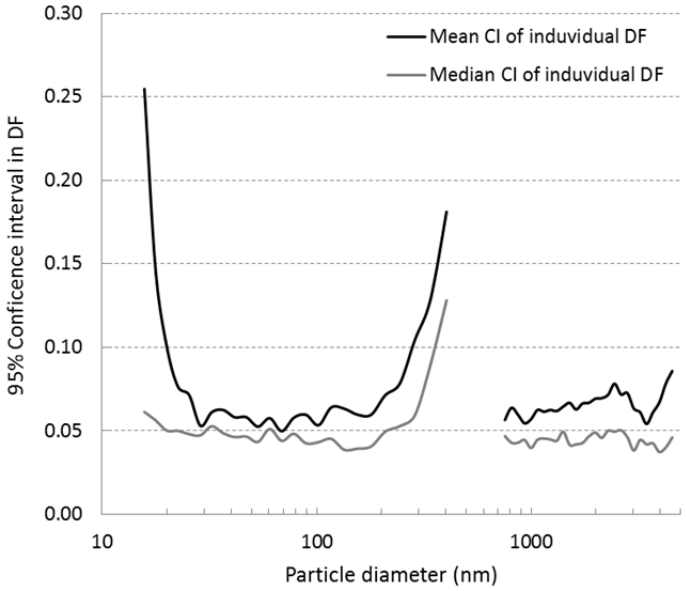

Fig. 6. The average and median confidence intervals for the individual DF curves. Note that this is a measure of the average uncertainty of all individual DF curves and not of the uncertainty in the DF average curve (shown in Fig. 2).

indicate that at normal breathing, inertial impaction becomes significant for particles > 3500 nm. The design of the set-up, with an SMPS classifying particles of 15–500 nm and an APS for particles > 800 nm, makes the measured DF independent of particle shape and density (fibers and elongated aggregates aligning in the DMA or in the accelerating flow of the APS excepted). This is contrary to when using optical sizing techniques based on static light scattering where particle density and shape is needed to estimate the corresponding aerodynamic particle diameter.

We report trends in the deposited particle levels between different subpopulations within the adult group. For example, a trend of decreasing deposition efficiencies with age was found. However, most individual variation was neither explained by age nor by gender, but by breathing pattern and lung intrinsic properties (investigated in more detail in a separate study: Rissler *et al.* [2017]). The results showed that some individuals within the group did receive doses twice as high as those of others when exposed to the same particle levels, as was also observed in the study by Löndahl *et al.* (2007). This can be part of the explanation as to why some individuals seem to be more susceptible to air pollution than others. The measured DF was applied to two model aerosols representing the aerosol found at an urban and a rural site, and the absolute deposition rates were derived. The deposition rates were also normalized to lung surface area and body mass, resulting in similar observations as those described for DF – with the exception of the children.

Children have been identified as a potentially sensitive group to air pollution, and efforts have been made to understand the particle deposition in the lungs of children (e.g., Smith *et al.*, 2001; Asgharian, 2004; Bennett and Zeman, 2004; Olvera *et al.*, 2012). In this study we found that for children, DF, TDF, and Drate were generally higher than for the adult group. However, the difference was statistically significant only for Drate, which was around 20% higher in the group of children compared to the adults. This was when the subjects were sitting in a relaxed position. Considering the typically higher activity level of children, one could expect that the average minute ventilation would be higher than when sitting still, and thus the real-life difference in Drate between children and adults is expected to be larger than reported here. When normalizing the deposition rate to lung surface area or body mass, the average dose of the children was more than double that of the average dose of the adults, and varied considerably more within the group of children than within the group of adults. The normalized dose measures are expected to be closely related to the inflammatory response and thus, this makes children a group that is highly susceptible to air pollution.

ACKNOWLEDGMENTS

This research was supported by the Swedish Governmental Agency for Innovation Systems, VINNOVA (Project 2009-01117), the Swedish Research Council for Environmental, Agricultural Sciences and Spatial Planning, FORMAS (Project 2009-1294) and the Swedish Research Council (Project 621-2011-3560). We gratefully thank Bo Olsson (Emmace Consulting AB, Södra Sandby, Sweden) for the help with modelling the DF.

SUPPLEMENTAL INFORMATION

The Supplemental Material contains (*i*) more details on the experimental set-up and (*ii*) supplemental figures of the $RESPI_2$, system particle losses, individual $DF(d_p)$ curves, the experimental set-up for particle generation, size distributions, and the error in DF due to a theoretical size shift.

Supplementary data associated with this article can be found in the online version at http://www.aaqr.org.

DISCLAIMER

The authors declare they have no competing interests.

REFERENCES

Anjilvel, S. and Asgharian, B. (1995). A multiple-path model of fiber deposition in the rat lung. *Fundam. Appl. Toxicol.* 28: 41–50.

Asgharian, B. (2004). A model of deposition of hygroscopic particles in the human lung. *Aerosol Sci. Technol.* 38: 938–947.

Becquemin, M.H., Yu, C.P., Roy, M. and Bouchikhi, A. (1991). Total deposition of inhaled particles related to age: Comparison with age-dependent model calculations.. *Radiat. Prot. Dosim.* 38: 23–28.

Bennett, W.D., Zeman, K.L. and Kim, C. (1996). Variability of fine particle deposition in healthy adults: Effect of age and gender. *Am. J. Respir. Crit. Care Med.* 153: 1641–1647.

Bennett, W.D., Zeman, K.L., Kim, C. and Mascarella, J. (1997). Enhanced deposition of fine particles in COPD patients spontaneously breathing at rest. *Inhalation Toxicol.* 9: 1–14.

Bennett, W.D. and Zeman, K.L. (1998). Deposition of fine particles in children spontaneously breathing at rest. *Inhalation Toxicol.* 10: 831–842.

Bennett, W.D. and Zeman, K.L. (2004). Effect of body size on breathing pattern and fine-particle deposition in children. *J. Appl. Physiol.* 97: 821–826.

Brown, J.S., Zeman, K.L. and Bennett, W.D. (2002). Ultrafine particle deposition and clearance in the healthy and obstructed lung. *Am. J. Respir. Crit. Care Med.* 166: 1240–1247.

Chalupa, D.C., Morrow, P.E., Oberdorster, G., Utell, M.J. and Frampton, M.W. (2004). Ultrafine particle deposition in subjects with asthma. *Environ. Health Perspect.* 112: 879–882.

Chan, T.L. and Lippmann, M. (1980). Experimental measurements and empirical modelling of the regional deposition of inhaled particles in humans. *Am. Ind. Hyg. Assoc. J.* 41: 399–408.

Cuddihy, R.G., Fisher, G.L. and Phalen, R.F. (1997). Deposition, retention and dosimetry of inhaled radioactive substances, In *NCRP Report*, pp. 1–225.

Daigle, C.C., Chalupa, D.C., Gibb, F.R., Morrow, P.E., Oberdorster, G., Utell, M.J. and Frampton, M.W. (2003). Ultrafine particle deposition in humans during rest and exercise. *Inhalation Toxicol.* 15: 539–552.

Dautrebande, L., Beckmann, H. and Walkenhorst, W. (1959). Studies on deposition of submicronic dust particles in the respiratory tract. *AMA Arch. Ind. Health* 19: 383–391.

Giacomelli-Maltoni, G., Melandri, C., Prodi, V. and Tarroni, G. (1972). Deposition efficiency of monodisperse particles in human respiratory tract. *Am. Ind. Hyg. Assoc. J.* 33: 603–610.

Heyder, J., Armbruster, L., Gebhart, J., Grein, E. and Stahlhofen, W. (1975). Total deposition of aerosol particles in the human respiratory tract for nose and mouth breathing. *J. Aerosol Sci.* 6: 311–328.

Heyder, J., Gebhart, J., Stahlhofen, W. and Stuck, B. (1982). Biological variability of particle deposition in the human respiratory tract during controlled and spontaneous mouth-breathing. *Ann. Occup. Hyg.* 26: 137–147.

Heyder, J., Gebhart, J., Rudolf, G., Schiller, C.F. and Stahlhofen, W. (1986). Deposition of particles in the human respiratory tract in the size range 0.005–15 μm. *J. Aerosol Sci.* 17: 811–825.

Hinds, W. (1999). *Aerosol Technology*, 2nd ed. John Wiley & Sons, Inc.

ICRP (1994). Human Respiratory Tract Model for Radiological Protection, In Annals of the ICRP.

Isaacs, K.K. and Martonen, T.B. (2005). Particle deposition in children's lungs: Theory and experiment. *J. Aerosol Med.* 18: 337–353.

Kim, C.S. and Jaques, P.A. (2005). Total lung deposition of ultrafine particles in elderly subjects during controlled breathing. *Inhalation Toxicol.* 17: 387–399.

Kim, C.S., Lewars, G.A. and Sackner, M.A. (1988). Measurement of total lung aerosol deposition as an index of lung abnormality. *J. Appl. Physiol.* 64: 1527–1536.

Landahl, H.D. and Herrmann, R.G. (1948). On the retention of airborne particulates in the human lung. *J. Ind. Hyg. Toxicol.* 30: 181–188.

Löndahl, J., Pagels, J., Swietlicki, E., Zhou, J.C., Ketzel, M., Massling, A. and Bohgard, M. (2006). A set-up for field studies of respiratory tract deposition of fine and ultrafine particles in humans. *J. Aerosol Sci.* 37: 1152–1163.

Löndahl, J., Massling, A., Pagels, J., Swietlicki, E., Vaclavik, E. and Loft, S. (2007). Size-resolved respiratory-tract deposition of fine and ultrafine hydrophobic and hygroscopic aerosol particles during rest and exercise. *Inhalation Toxicol.* 19: 109–116.

Löndahl, J., Swietlicki, E., Rissler, J., Bengtsson, A., Boman, C., Blomberg, A. and Sandström, T. (2012). Experimental determination of the respiratory tract deposition of diesel combustion particles in patients with chronic obstructive pulmonary disease. *Part. Fibre Toxicol.* 9: 30.

Löndahl, J., Möller, W., Pagels, J.H., Kreyling, W.G., Swietlicki, E. and Schmid, O. (2014). Measurement techniques for respiratory tract deposition of airborne nanoparticles: A critical review. *J. Aerosol Med. Pulm. Drug Deliv.* 27: 229–254.

Melandri, C., Tarroni, G., Prodi, V., Dezaiacomo, T., Formignani, M. and Lombardi, C.C. (1983). Deposition of charged-particles in the human airways. *J. Aerosol Sci.* 14: 657–669.

Möller, W., Felten, K., Sommerer, K., Scheuch, G., Meyer, G., Meyer, P., Haussinger, K. and Kreyling, W.G. (2008). Deposition, retention, and translocation of ultrafine particles from the central airways and lung periphery. *Am. J. Respir. Crit. Care Med.* 177: 426–432.

Montoya, L.D., Lawrence, J., Murthy, G.G.K., Sarnat, J.A., Godleski, J.J. and Koutrakis, P. (2004). Continuous measurements of ambient particle deposition in human

subjects. *Aerosol Sci. Technol.* 38: 980–990.

Morrow, P.E. (1986). Factors determining hygroscopic aerosol deposition in airways. *Physiol. Rev.* 66: 330–376.

Olvera, H.A., Perez, D., Clague, J.W., Cheng, Y.S., Li, W.W., Amaya, M.A., Burchiel, S.W., Berwick, M. and Pingitore, N.E. (2012). The effect of ventilation, age, and asthmatic condition on ultrafine particle deposition in children. *Pulm. Med.* 2012: 736290.

Rissler, J., Swietlicki, E., Bengtsson, A., Boman, C., Pagels, J., Sandström, T., Blomberg, A. and Löndahl, J. (2012). Experimental determination of deposition of diesel exhaust particles in the human respiratory tract. *J. Aerosol Sci.* 48: 18–33.

Rissler, J., Nordin, E.Z., Eriksson, A.C., Nilsson, P.T., Frosch, M., Sporre, M.K., Wierzbicka, A., Svenningsson, B., Löndahl, J., Messing, M.E., Sjogren, S., Hemmingsen, J.G., Loft, S., Pagels, J.H. and Swietlicki, E. (2014). Effective density and mixing state of aerosol particles in a near-traffic urban environment. *Environ. Sci. Technol.* 48: 6300–6308.

Rissler, J., Gudmundsson, A., Nicklasson, H., Swietlicki, E., Wollmer, P. and Löndahl, J. (2017). Deposition efficiency of inhaled particles (15-5000 nm) related to breathing pattern and lung function: An experimental study in healthy children and adults. *Part. Fibre Toxicol.* 14: 10.

Rosati, J.A., Brown, J.S., Peters, T.M., Leith, D. and Kim, C.S. (2002). A polydisperse aerosol inhalation system designed for human studies. *J. Aerosol Sci.* 33: 1433–1446.

Schiller, C.F., Hlawa, R., Gebhart, J., Wönne, R. and Heyder, J. (1992). Total deposition of aerosol particles in the respiratory tract of children during spontaneous and controlled mouth breathing. *J. Aerosol Sci.* 23: 457–460.

Schiller-Scotland, C.F., Hlawa, R. and Gebhart, J. (1994). Experimental-data for total deposition in the respiratory-tract of children. *Toxicol. Lett.* 72: 137–144.

Schiller-Scotland, C.F., Gebhart, J., Hochrainer, D. and Siekmeier, R. (1996). Deposition of inspired aerosol particles within the respiratory tract of patients with obstructive lung disease. *Toxicol. Lett.* 88: 255–261.

Schmid, O., Bolle, I., Harder, V., Karg, E., Takenaka, S., Schulz, H. and Ferron, G.A. (2008). Model for the deposition of aerosol particles in the respiratory tract of the rat. I. Nonhygroscopic particle deposition. *J. Aerosol Med. Pulm. Drug Deliv.* 21: 291–307.

Schmid, O. and Stoeger, T. (2016). Surface area is the biologically most effective dose metric for acute nanoparticle toxicity in the lung. *J. Aerosol Sci.* 99: 133–143.

Smith, S., Cheng, U.S. and Yeh, H.C. (2001). Deposition of ultrafine particles in human tracheobronchial airways of adults and children. *Aerosol Sci. Technol.* 35: 697–709.

van Wijk, A.M. and Patterson, H.S. (1940). The percentage of particles of different sizes removed from dust-laden air by breathing. *J. Ind. Hyg. Toxicol.* 22: 31–35.

Weibel, E.R. (1963). *Morphometry of the Human Lung*. Springer Verlag and Academic Press, Berlin, New York.

Wiebert, P., Sanchez-Crespo, A., Falk, R., Philipson, K., Lundin, A., Larsson, S., Moller, W., Kreyling, W.G. and Svartengren, M. (2006a). No significant translocation of inhaled 35-nm carbon particles to the circulation in humans. *Inhalation Toxicol.* 18: 741–747.

Wiebert, P., Sanchez-Crespo, A., Seitz, J., Falk, R., Philipson, K., Kreyling, W.G., Moller, W., Sommerer, K., Larsson, S. and Svartengren, M. (2006b). Negligible clearance of ultrafine particles retained in healthy and affected human lungs. *Eur. Respir. J.* 28: 286–290.

Wierzbicka, A., Nilsson, P.T., Rissler, J., Sallsten, G., Xu, Y., Pagels, J.H., Albin, M., Österberg, K., Strandberg, B., Eriksson, A., Bohgard, M., Bergemalm-Rynell, K. and Gudmundsson, A. (2014). Detailed diesel exhaust characteristics including particle surface area and lung deposited dose for better understanding of health effects in human chamber exposure studies. *Atmos. Environ.* 86: 212–219.

Yeh, H.C. and Schum, G.M. (1980). Models of human-lung airways and their application to inhaled particle deposition. *Bull. Math. Biol.* 42: 461–480.

Yu, C.P. and Diu, C.K. (1982). A Comparative study of aerosol deposition in different lung models. *Am. Ind. Hyg. Assoc. J.* 43: 54–65.

Received for review, September 28, 2016
Revised, January 12, 2017
Accepted, January 18, 2017